Enhancement of Optical Properties of Borate Glass Doped with Vanadium Oxide

S A Abdel Gawad[1], A N EL-Sharkawy[1], K R Mahmoud[2], A M A Henaish[3,4]*, O M Hemeda[4] and Ahmed R Ghazy[4]

[1]Department of Physics, Misr University for Science and Technology, Egypt

[2]Department of Physics, Kafr elsheikh University, Egypt

[3]Ural Federal University, Nanotech Center, Russia

[4]Department of Physics, Tanta University, Egypt

Submitted: February 06, 2022; **Published:** February 24, 2022

*Corresponding author: A M A Henaish, Ural Federal University, Nanotech Center, Russia, Department of Physics, Tanta University, Egypt

Abstract

In this work we examine physical, structural and optical properties of borate glass via experimental and theoretical techniques. The composition of our glass samples is $(50-X)$ B_2O_3 + 50 Pb_3O_4 + X V_2O_5 encoded into [BPV glass system] where x= (0, 0.1, 0.2, 0.3, 0.4 and 0.5) were prepared using melt quenching method. X-ray diffraction technique confirmed the formation of BPV glass system. Characteristic absorption bands were observed in infrared spectra assigned to vibrational modes. The optical properties of the prepared samples were measured using UV-visible spectra and Photoluminescence. The optical energy band gap E_g (direct and indirect) calculated using Tauc,s equation and found that direct energy gap decreases from 2.42 ev to 2.26 ev and indirect energy gap decreases from 2.57 ev to 2.52 ev as vanadium oxide increase and that Urbach energy Eu decreased from 0.21 ev to 0.18 ev. The refractive index increased by V_2O_5 content increased and steepness parameter increased also. The dielectric constant (ε) and optical conductivity (σ) have the same behavior decrease by increasing vanadium oxide content. Photoluminescence shows an emission wavelength that ranges from 400 nm to 1000 nm.

Keywords: Borate glass; Vanadium oxide; XRD; FTIR; Urbach energy; Photoluminescence

Abbreviations: FTIR: Fourier Transformer Infrared; XRD: X-Ray Diffraction; UV: Ultraviolet Spectroscopy; PL: Photoluminescence; VELF: Volume Energy Loss Function; SELF: Surface Energy Loss Function

Introduction

Glasses are inorganic material come from fusion that has cooled to super cooled liquids, transparent, rigid and amorphous product. For several years the nature of glass was attracted to be studied because of their electronic and optical behavior of different types of glasses. Borate glass is a special material because of bond formation is very strong, reduces thermal expansion, increase toughness and lowering melting point temperature which help to benefits from the properties of glasses at suitable temperature that can be easy to deal with [1-3]. Some of the different borate glass applications is optical fibers and filters, communication and laser or γ-ray attenuation devices [1,4,5]. Glasses containing vanadium oxide is very important because it give the glass some of n-type semiconductor material that return to the nature of vanadium atom that has unpaired electron move between different band states e.g. V^{4+} and V^{5+} [6,7]. This behavior helps in many applications that need superconductor character like material forming cathode or in battery usage. The borate glass system we have consist of different V_2O_5 concentration added on account of B_2O_3 and constant value of Pb_3O_4. In lead vanadate glasses fourfold coordinated vanadium $[VO_4]^+$ and five sour coordinated vanadium$[Vo_5]$ which form various types of units $[V_2O_7]^{4-}$ and $[V_2O_8]_n$ zigzag chin [3,5]. In general, the B_2O_3 is good glass formed and found in two ways of boron reported three coordinated boron $[BO_3]$ and four coordinated boron $[BO_4]$, the three coordinated boron found in our used boron which is B_2O_3 glass. When added other oxide we called glass modifier. The transition of borate glass bond formation reflects the change of superstructure units. Also, the lead borate glass Pb_3O_4 showing change in boron superstructure changes as lead oxide content increase. So, we have various changes in the glass system depend on the main component borate glass or other oxides which is added to it that help to give it a variety in the structure which make a development in many applications that can be useful b understanding the behavior. The x-ray diffraction (XRD) was studied to ensure the amorphous and disordered features of glass

formed. The study of different optical properties such as the FTIR, UV and PL to study the amorphous nature and determine the different optical parameter. FTIR (Fourier transformer infrared) is the more effective tool to study the amorphous nature and character the absorption peaks at specific wave number for glass materials. UV (ultraviolet spectroscopy) help to have the optical properties of the glass samples by determine the optical band gap, absorption peaks, refractive index and optical conductivity. PL (Photoluminescence) to study the structure changes taking place in the glass system due to the doping concentration. The aim of the present work is to investigate the borate glass with different concentration of vanadium oxide samples have different optical properties using a variable measurement in order to analysis how the vanadium oxide can play a role on the vibrational and optical properties of borate glasses.

Experimental

Sample preparation

Glass samples with chemical composition of $(50-x)$ B_2O_3 +50 Pb_3O_4 + X V_2O_5 [BPV glass system] where x= (0, 0.1, 0.2, 0.3, 0.4 and 0.5) were prepared using the melt and quench method. The weighted precursors were fully mixed to get uniform compositional mixture and finely ground taken in porcelain crucibles kept inside the electric furnace for melting. The glass blends were maintained at temperature $800^{\circ}C$ about 20 min. The prepared glasses were suddenly molded at $200^{\circ}C$ using a stainless-steel pattern to take shape in discs form (Figure 1). The molecular weights of the different samples of BPV glass system shown in Table 1.
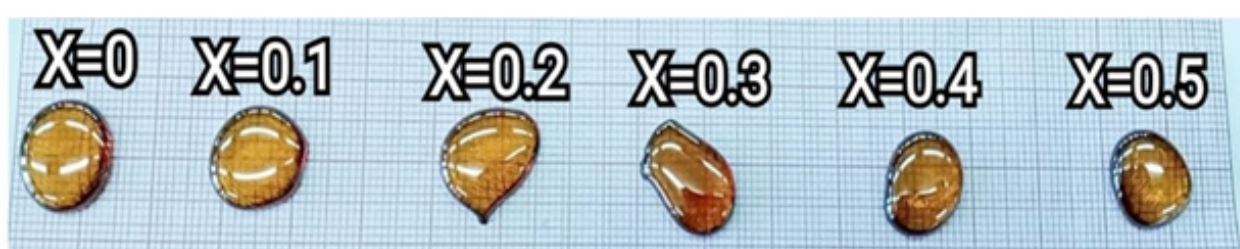

Figure 1: The prepared glass samples of BPV glass system.

Table 1: The weights of the different sample of BPV glass system.

Sample	Chemical Composition, wt%		
	B_2O_3	Pb_3O_4	V_2O_5
BPV_0	50	50	0
$BPV_{0.1}$	49.9	50	0.1
$BPV_{0.2}$	49.8	50	0.2
$BPV_{0.3}$	49.7	50	0.3
$BPV_{0.4}$	49.6	50	0.4
$BPV_{0.5}$	49.5	50	0.5

Sample characterization

The amorphous character of prepared glasses was confirmed using X-ray diffraction (XRD) technique with Cu K_α radiation source (λ=1.54nm) Philips model (PW-1729) step size $0.02^{\circ}C$; time per step: 21 sec. The optical properties of the samples were also characterized using FTIR spectrometer by using a PERKIN-ELMER-1430 recording infrared spectra in the range 200 to 4000cm^{-1}. The UV/visible spectrum of the prepared glasses using V-630 UV-Vis Spectrophotometer with double-beam spectrophotometer have single monochromator. Silicon photodiode detectors. Range 190 to 1100 nm Fixed bandpass of 1.5 nm. High-speed scanning up to 8,000 nm/min.

Photoluminescence (PL) He Cd laser (325nm and 150mW) is directed onto the sample When the laser beam is incident on the sample, photoluminescence occurs and light is emitted from the sample at wavelengths dependent on the sample composition. The sample is oriented such that the reflected laser beam and the PL emission propagate in different directions. The emitted light is directed into a fiber optic cable and then into a spectrometer. A filter may be placed in front of the fiber input to remove any incident laser light. Inside the spectrometer, a diffraction grating diffracts different wavelengths in different directions towards an array of photo-detectors that measure the intensity of each wavelength component. The digital information is interpreted by the computer, which can display a PL spectrum. The spectrum indicates the relative intensities of light of different wavelengths entering the detector.

Results and Discussion

X-ray diffraction (XRD)

The X-ray diffraction (XRD) used to identify the crystalline phase of transparent samples. The amorphous crystalline nature of glass sample is confirmed by XRD. It gives us information of the type of our material according to the distribution of the atoms relative to each other as well as the length scale over which the crystalline order persists. The XRD pattern of the BPV glass system is shown in Figure 2. The Figure provided that the amorphous and disorder features of the BPV glass samples and confirmed the formation of the glass system. As shown in the Figure there is an

only peak at 30°C which its intensity was increased by increasing V_2O_5 content. XRD show absence of any other sharp crystalline peaks which confirm the amorphous and noncrystalline nature of BPV glass system [8,9]. The intensity of the peak increased by increasing of V_2O_5 content but there is no shift in this peak and we don't mention the intensity because we only confirmed the amorphous crystalline nature of the material and the intensity values shown in Table 2.
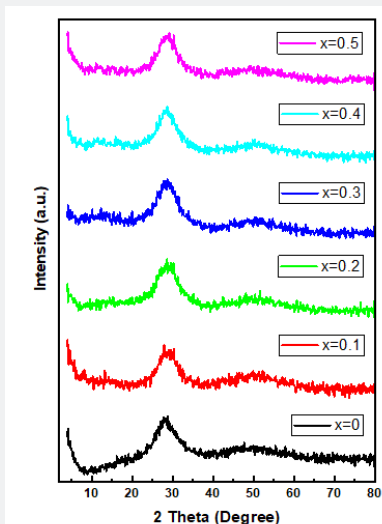
Figure 2: The XRD pattern of glass samples for various V_2O_5 concentrations.

Table 2: The change in intensity value with V_2O_5 content.

V_2O_5 Content	Intensity (a.u.)
0	214
0.1	220
0.2	272
0.3	283
0.4	294
0.5	268

Infrared spectrum (FTIR)

For studying the molecular structure and dynamics of the investigated glasses, FTIR spectra were recorded between 200-4000cm^{-1} are shown in Figure 3. As shown in Figure 3 The glass compositions show six absorption bands and these peaks positions are assigned to various vibrational modes. The weak reflection at 545 cm^{-1} can be attributed to $V^{+5} – O^{2-}$, Pb^{+3}_ O^{2-} the metallic content [4,10,11]. That band near (830-725 cm^{-1}) is characteristic of Diborate linkage B_O_B inside the borate glassy network [12-14]. The stretching vibration at (1147-952 cm^{-1}) is due to B_O_V^{+5} and B_O_Pb^{+3}[13,15]. The band located around 1530 cm^{-1} is characteristic of anti-symmetric stretching vibration of [BO$_3$][16]. Asymmetric stretching relaxation of B_O bonds of trigonal BO3 units at around (1741-1636 cm^{-1}) [17,18]. The band at 3500 cm^{-1} is due to the vibration of H_2O molecule [1,19]. The main absorption bands and the corresponding vibration modes of FTIR spectra of the studied glasses represented in Table 3.

Table 3: Peak position of IR assignment.

Peak Positions (cm^{-1})	IR Assignments	References
3450	Related to water molecular vibration.	[1]
1741-1636	Asymmetric stretching relaxation of B_O bonds of trigonal BO$_3$ units	[17,18]
1530	Related to the vanadium content	[16]
1147-952	Stretching vibration of B_O_V^{+5} and B_O_Pb^{+3}	[13]
830-725	Diborate linkage B_O_B inside the borate glassy network	[12-14]
545	V^{+5}, Pb^{+3} the metallic content	[10,11]

Optical properties

UV-visible absorption spectrum: The UV-visible absorption spectrum of the glass series (50-x) B_2O_3 +50 Pb_3O_4 + X V_2O_5 where x= (0, 0.1, 0.2, 0.3, 0.4 and 0.5) are shown in Figure 4. The absorption band stretches from 429-452 nm is recognized with π-π* electronic transition [20]. The second peak located at

λ=419.4nm is corresponding to the band gap energy, and it can observe that the second peak shifted to a higher wavelength by increasing V2O5 concentration. This concerning to the structural rearrangement of the glass matrix and the modifier [8,21]. It was also regarded to the changes in bonding in the glassy network as the metal content was increased [22,23]. The optical parameter of borate glass doped with different content of V_2O_5 (0, 0.1, 0.2, 0.3, 0.4 and 0.5) were studied. The absorption spectra were measured for all glass samples at the range from 400-800 nm. We recalculate the absorption coefficient α from another equation [24]:
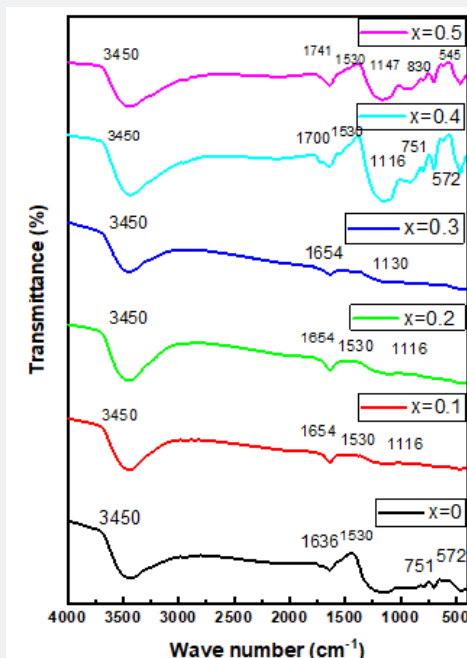

Figure 3: FTIR of glass samples for various V_2O_5 concentrations.

$$\alpha(\lambda) = 2.303\left(\frac{A}{d}\right)$$

Where A: is the material absorbance and d is the thickness of the material.

α shows an increasing behavior with incident photon energy as shown in Figure 5. On the other hand, it increases as vanadium content increase up to x=0.3 and then decrease for x=0.4 and =0.5. In general, the absorption coefficient for doped glass samples are higher than the undoped one. This increase in absorption coefficient make the possibility of the doped glass samples to be used as absorption layer in solar cell specially the sample x=0.3. The UV absorption band is observed to be shifted to higher wavelength by increasing of V_2O_5 content. $BPV_{0.1}$ has more obvious peaks at λ=404.849nm and the second peak at λ=431.325nm. While $BPV_{0.2}$ and $BPV_{0.3}$ compact the peaks into shoulder which is located at wavelength λ=443.949nm and λ=452.546nm respectively. Then suddenly the peak changes their positions to lower wavelengths at samples $BPV_{0.4}$ and $BPV_{0.5}$, at $BPV_{0.4}$ it shows shoulder at around wavelength λ=451.8nm and $BPV_{0.5}$ shows appearance of the two peaks again at wavelengths λ=406.1nm and λ=431.2nm as shown in Figure 5. The optical absorption coefficient of the BPV glass samples for different concentration of V_2O_5 shown at Figure 5. The optical absorption coefficient of BPV0 at α=11.7 cm^{-1} then shift to higher values by increasing of V_2O_5 content in the glass samples firstly BPV0.1 at α=14.2 cm^{-1}, $BPV_{0.2}$ at α=14.4 cm^{-1}, BPV0.3 at α=22.5 cm^{-1} then the optical absorption coefficient changes their positions again to lower values at the two samples $BPV_{0.4}$ at α=18.8 cm^{-1} and $BPV_{0.5}$ at α=14.03 cm^{-1}. The presence of V_2O_5 in the glass system(50-x) B_2O_3 +50 Pb_3O_4 + X V_2O_5 where x= (0, 0.1, 0.2, 0.3, 0.4 and 0.5) with different values content affect the particle size values and change it to very small values at x=0.3 equal 8.58 nm and then increase again at x=0.5 to 28.02 nm. The maximum absorption occur at x=0.3due to its very small particle size which give a spread area to absorb more light and enhance the absorption coefficient. The sample x=0.5 has the largest value particle size which lead to the decrease of the absorption coefficient again and become near to the value of 0.1 V_2O_5 as shown in Table 4.

The extension coefficient(K) is investigated in Figure 6 using the following equation [20,25]:

$$K = \frac{\alpha\lambda}{4\Pi}$$

Where α: the absorption coefficient, λ: is wavelength.

The Figure 6 shows the dependence of K on photon energy for all glass samples. It can be seen that K decrease with incident photon energy conversely the absorption coefficient whereas increase by increasing vanadium oxide content in the range of wavelength from 400-550 nm.
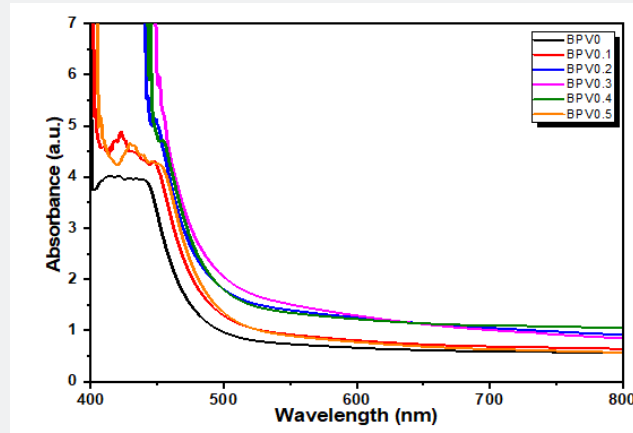
Figure 4: UV-visible absorption spectrum of the investigated glass samples for different concentration of V_2O_5.
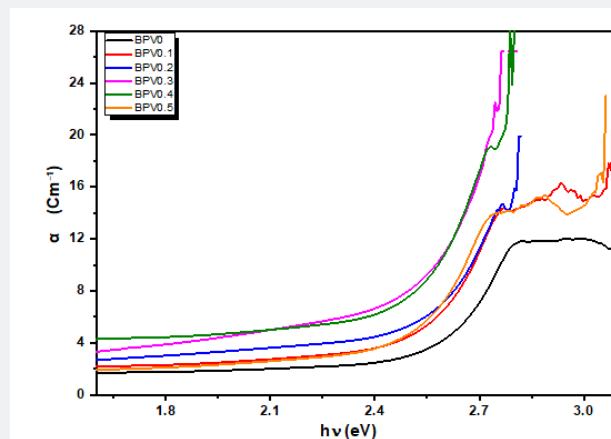
Figure 5: optical absorption coefficient of the investigated glass samples for different concentration of V_2O_5.
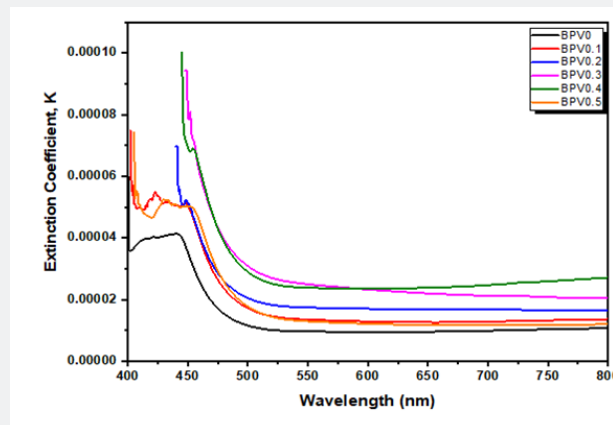
Figure 6: The dependence of extinction coefficient (K) of the investigated glass samples for different concentration of V_2O_5 on the wavelength λ(nm).

Table 4: The change in particle size with vanadium oxide content.

V_2O_5 Content	Particle Size (nm)
0	16.68
0.3	8.58
0.5	28.02

The optical band gap E_g can be obtained from the plot

$(\alpha h\nu)^{\frac{1}{2}}$ and $(\alpha h\nu)^2$ versus hν indirect and direct transition using the following expression [26,27]:

$$(\alpha h\nu)^n = cons\tan t(h\nu - E_g)$$

Which are a parameter describe the transition type. The value of n indicate the type of transition and it equals 2 or $\frac{1}{2}$ for direct and indirect allowed transition respectively as shown in Figure 7. The calculated values of direct and indirect band gap are given in Table 5. The values of optical activation energy decrease b increasing vanadium content of direct and indirect transition which mean that the optical conductivity increase by increasing vanadium oxide content up to x=0.3.
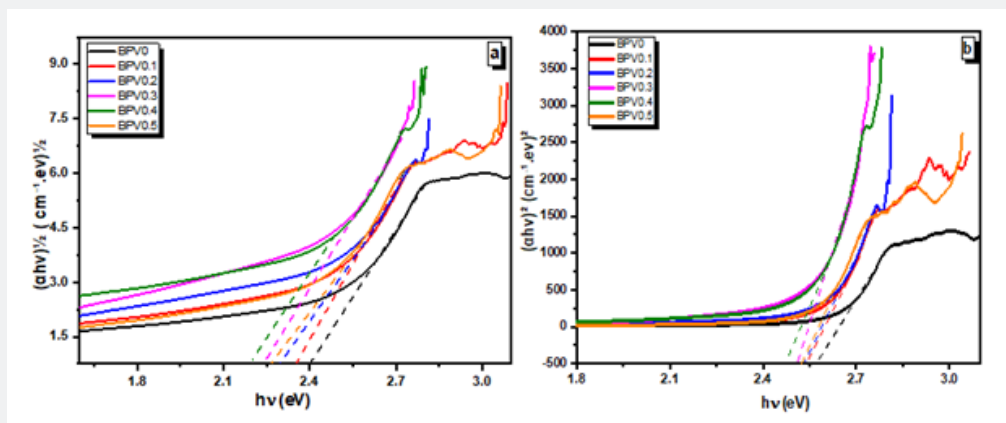
Figure 7: The dependence of (a) $(\alpha h\nu)^{1/2}$ and (b) $(\alpha h\nu)^2$ on photon energy (hν) of the investigated glass samples for different concentration of V_2O_5.

Table 5: Optical parameters values for the BPV glass system.

| Sample	E_g (ev) (Direct)	E_g (ev) (Indirect)	EU (ev)	n
BPV_0	2.42	2.57	0.21	3.58
$BPV_{0.1}$	2.35	2.54	0.19	4.05
$BPV_{0.2}$	2.31	2.53	0.21	5.77
$BPV_{0.3}$	2.24	2.51	0.22	5.56
$BPV_{0.4}$	2.19	2.47	0.21	5.97
$BPV_{0.5}$	2.26	2.52	0.18	3.76

The optical band gap has two main optical transitions (direct and indirect transitions) can be detected below and near the fundamental absorption edge. The electromagnetic waves interact with electrons in the valence band and moves to the conduction band through the fundamental gap. In the case of glass, the glass forming anions effects on the conduction band and cations play a key role in indirect band transition [28,29].

The direct and indirect energy gaps are tabulated in Table 5 & Figure 8 describes $\alpha h\nu^2$ and $\alpha h\nu^{1/2}$ with hν for the direct and indirect allowed transitions for the BPV glass system. The energy band gap decreases by increasing of V_2O_5 content direct and indirect as shown in Table 5. The Urbach relation can be describe the absorption coefficient in the region exponential energy [9,28]:

$$\alpha = \alpha_o e^{h\nu/E_u}$$

Where: α, αo, and E_u are the absorption coefficient, constant, and Urbach energy. The relation between ln (α) and hν is shown in Figure 8 from the slope of this fitting relation the value of Eu can be calculated and its value increase up to x=0.3 and then decrease at higher value. This was to evaluate the concentration of defects in the network of the BPV glass system. To determine the Urbach energy values, the reciprocals of the slopes of the linear region of curves are taken. The empirical Urbach rule gives the relationship between E_u and $\alpha(\nu)$, as is shown in equation [28,29]:
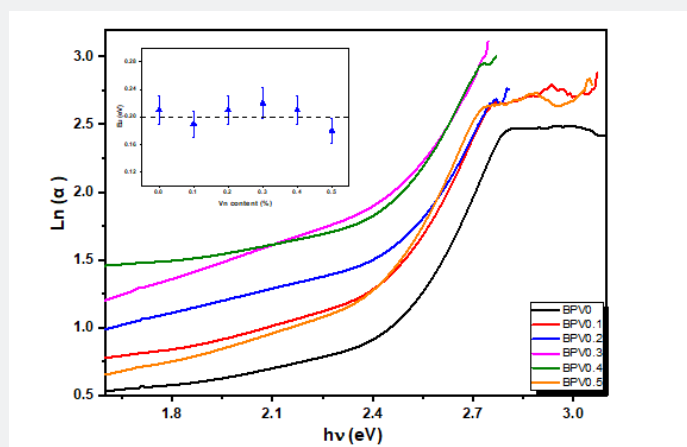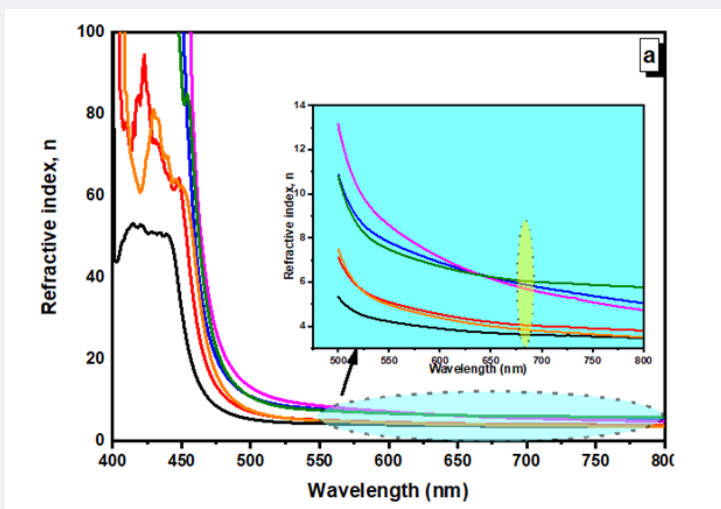
Figure 8: Plot of ln(α) with hν of the investigated glass samples for different concentration of V_2O_5 : the inset shows Eu as a function of V_2O_5 content.

$$Ln(\alpha) = Ln(\alpha_0) + \frac{h\nu}{E_u}$$

Where: α, αo, and E_u are the absorption coefficient, constant, and Urbach energy. The values of Urbach energy shown in Table 5.

The refractive index of the BPV glass samples was calculated by using the results of reflectance and transmittance according to the following relation [24,30]:

$$n = \left(\frac{1+R}{1-R}\right) + \left(\frac{4R}{(1-R)^2} - K^2\right)^{1/2}$$

Figure 9: The dependence of (a) refractive index (n) of the investigated glass samples for different concentration of V2O5 on the wavelength λ(nm).

Where R is the reflectance data, and k is the extinction coefficient. The values of the refractive index of BPV glass samples increases with increase of V_2O_5 except $BPV_{0.5}$ change in behavior. The refractive index as a function in wavelength shown in Figure 9 for all glass samples. The refractive index increase up to x=0.3 therefore the fabricated glass samples can be used as photovoltaic solar cells and optical devices.

The energy dispersion parameter for the refractive index is estimated using the Wemple and DiDomenico (WDD) single oscillator model [27,31]:

$$(n^2 - 1)^{-1} = \frac{E_0}{E_d} - \left(\frac{1}{E_0 E_d}\right)(h\nu)^2$$

where E_o is the single-oscillator energy (average of energy gap) and Ed the dispersion energy parameter, which measure the interband optical transition strength. Plotting vs. (hν)² provides straight lines that intercept the y-axis at (n²−1)⁻¹

E_o/E_d, giving a slope equal to $(-1/E_oE_d)$, as shown in Figure 10a. The calculated values of E_o and E_d are presented in Table 6. The values of E_0 decrease with increasing of vanadium content as we notice it has the same behavior as the optical energy gap. The value of E_d has an inverse performance which mean that dispersion energy increase by increasing of vanadium content.
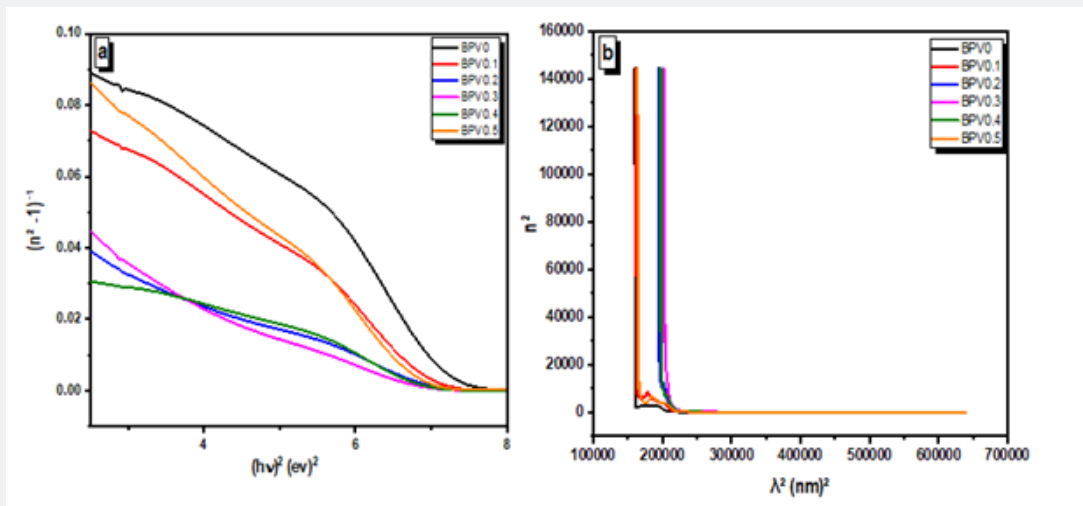
Figure 10: (a) $(n^2 - 1)^{-1}$ vs. the square of the photon energy $(hv)^2$ (b) (n2) vs. the square of the wavelength $(\lambda)^2$ of the investigated glass samples for different concentration of Pb_3O_4.

Table 6: values of steepness parameter (S), single oscillator energy (E_0), dispersion energy parameter (E_d), the dispersion refractive index (n_0) at zero energy photon (static refractive index), average oscillator wave length (λ_0) and average oscillator strength (S_0).

Sample	S	E_0 (ev)	E_d (ev)	n_0	λ_0(nm)	S_0(nm^{-2})
BPV$_0$	1.231	3.15	26.44	3.06	266.5	1.17×10^{-4}
BPV$_{0.1}$	1.361	2.83	26.7	3.23	311.45	0.972×10^{-4}
BPV$_{0.2}$	1.231	2.56	43.44	4.24	244.25	2.85×10^{-4}
BPV$_{0.3}$	1.175	2.39	32.27	3.81	499.89	0.541×10^{-4}
BPV$_{0.4}$	1.231	3.28	76.25	4.92	287.2	2.81×10^{-4}
BPV$_{0.5}$	1.436	2.73	21.32	2.97	318.19	0.772×10^{-4}

The dispersion refractive index (n_0) at zero energy photon (static refractive index) is calculated using equation [9,32]:

$$n_o^2 = \left(1 + \frac{E_d}{E_o}\right)$$

The value of n_o decrease with increase of vanadium content. Using the Moss model [9,33], we extracted the average oscillator wavelength (λ_0) values for the samples. The λ_0 value at minimum reflectance is given by the following equation [9,34]:

$$\frac{(n_o^2 - 1)}{(n^2 - 1)} = 1 - \left(\frac{\lambda_o}{\lambda}\right)2$$

Additionally, with the calculated λ_0 we can investigate the average oscillator strength (S_0) using equation [9,23]:

$$s_o = \frac{(n_o^2 - 1)}{\lambda_o^2}$$

The calculated λ_0 and S_0 values are shown in Table 6.

The study of the variation of optical dielectric constant $\varepsilon^\backslash$ and optical dielectric loss $\varepsilon^{\backslash\backslash}$ with photon energy of the studied glass samples BPV system shown in Figure 11. The Figure show that the real dielectric constant stay with constant value first then start to make a hump and final sudden increase of real dielectric constant with increase of photon energy as shown in Figure 12a. The imaginary dielectric constant has the same behavior of the real one as shown in Figure 12b.
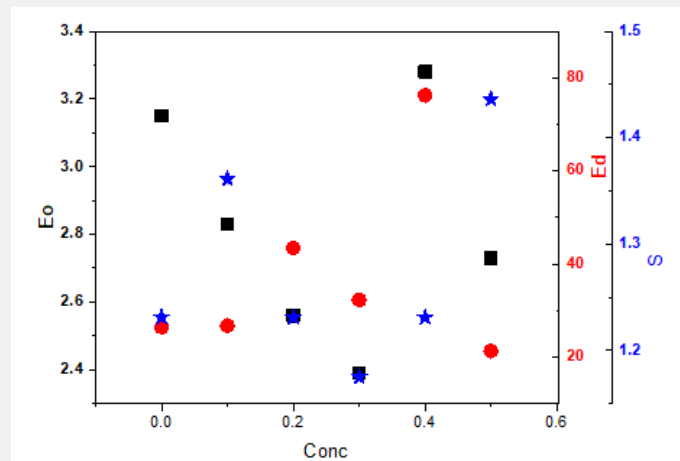
Figure 11: The variation of vanadium content with dispersion energy parameter (E_d), single oscillator energy (E_0) and values of steepness parameter (S).
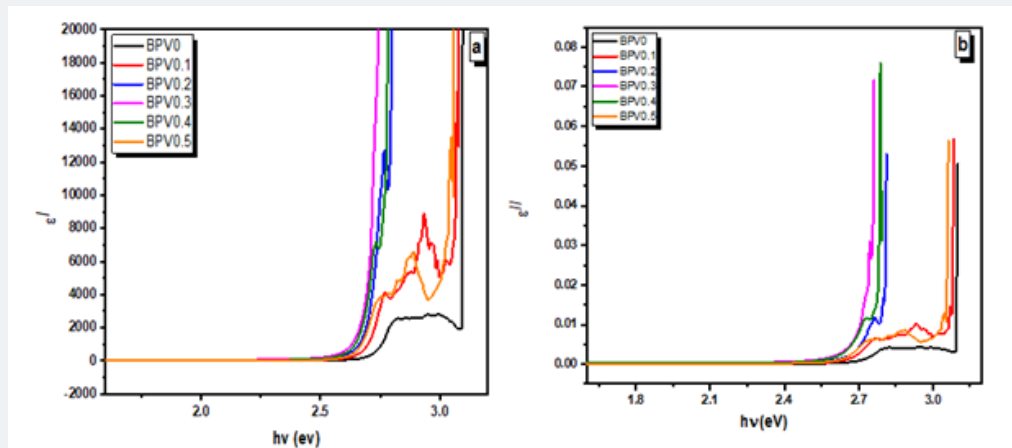
Figure 12: (a) Optical dielectric constant (ε'), (b): optical dielectric loss (ε") vs. photon energy of the investigated glass samples for different concentration of V_2O_5.
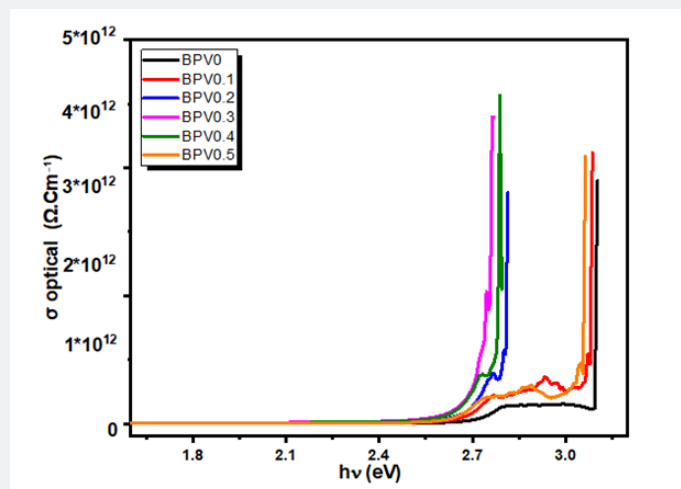
Figure 13: Optical conductivity vs. photon energy of the investigated glass samples for different concentration of V_2O_5.

The change of the optical conductivity (σ) with photon energy of the BPV glass system have the same behavior of dielectric constant which start with constant values first, then make a hump and finally a sudden increase of the optical conductivity with the increasing of photon energy values as shown in Figure 13. The σ optical and electrical can be specified by the following relation [17,28]:

$$\sigma_{optical} = \frac{\alpha(v)C_n}{4\Pi}$$

$$\sigma_{electrical} = \frac{2\lambda\sigma_{optical}}{\alpha(v)}$$

where α: absorbance depends on frequency, C: speed of light in vacuum. The quantities describe the energy loss rate for an electron passing through a material has been studied for the following BPV glass samples. The quantities known the volume energy loss function (VELF) and surface energy loss function (SELF) [27].

$$VELF = \frac{\varepsilon_2}{\varepsilon_1^2 + \varepsilon_2^2}$$

$$SELF = \frac{\varepsilon_2}{(\varepsilon_1+1)^2 + \varepsilon_2^2}$$

Where ε_1: real dielectric constant, ε_2: imaginary dielectric constant. The behavior of the physical quantities (VELF) and (SELF) decreases with increasing of photon energy as shown in Figure 13.

Photoluminescence

Photoluminescence spectrum show that the main peak around 523.6nm. The sample BPV0.4 is the higher intensity of all the samples and there is another peak around 703nm. The appearance of this peak due to deep level trap because of presence of vanadium which indicate the amount of vacancies in the samples at room temperature [6,24]. All the sample have constant acceptable vales of defect (Figure 14).
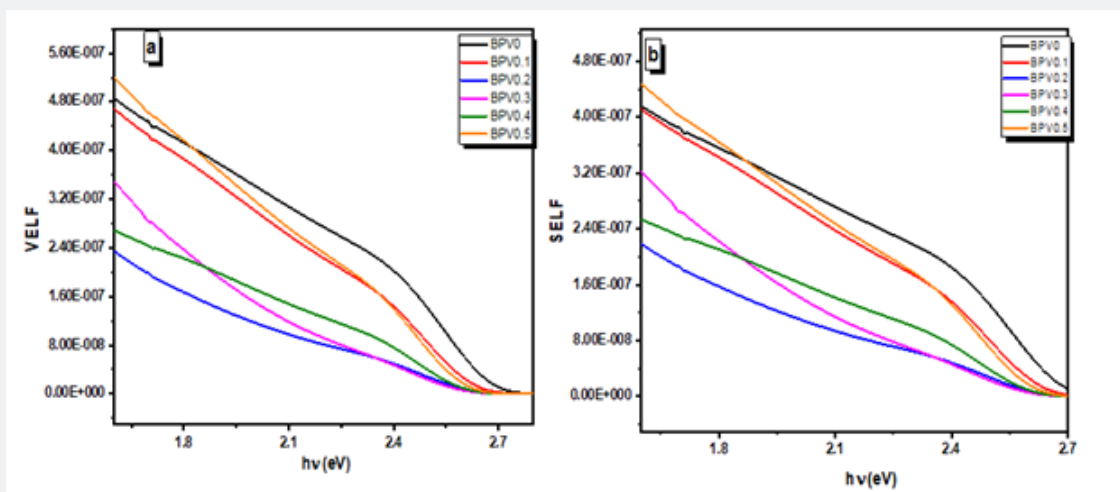

Figure 14: The dependence of the VELF and SELF of the investigated glass samples for different concentration of V_2O_5.

Table 7: Wavelength emission, stock shift and energy gap of photoluminescence of the BPV glass system.

Sample	λ_{em} (nm)	Stock Shift (cm^{-1})	E_g^{pl} (eV)
BPV0	522	0.43×10^4	2.38
BPV0.1	524.3	0.44×10^4	2.37
BPV0.2	522.7	0.44×10^4	2.37
BPV0.3	522.8	0.43×10^4	2.37
BPV0.4	520.9	0.43×10^4	2.38
BPV0.5	522.8	0.44×10^4	2.37

The emission spectrum of the BPV glass system shown in Figure 15 and the values of $\lambda_{emission}$ shown in Table 7. The value of E_g^{pl} (energy gap of Photoluminescence) is between 2.37 and 2.38 since the emission peak is at approximately constant wavelength value. The stock shift value related to the emitting fluorescence from molecules when the move between the emission and excitation state. The equation used to calculate stock shift [7,35]:

$$Stock \ \text{shift} \ \left(cm^{-1} \right) = 10^7 \left[\frac{1}{\lambda_{ex}(nm)} - \frac{1}{\lambda_{em}(nm)} \right]$$
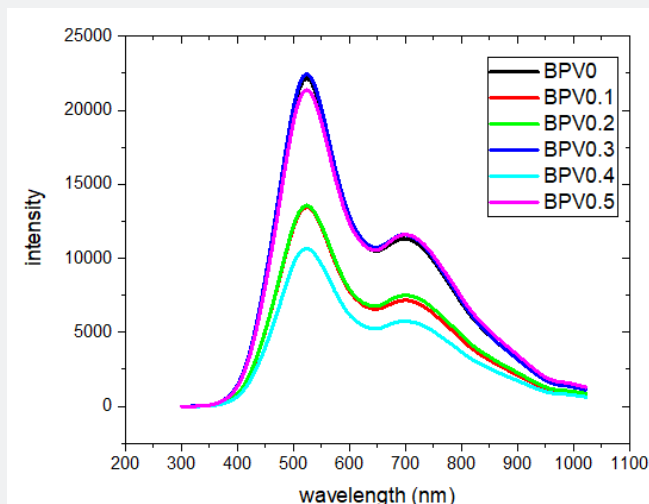

Figure 15: Photoluminescence Emission of BPV glass system with intensity.

Conclusion

The BPV glass system has an amorphous and disorder features which confirmed by the result of XRD since the absence of any sharp peaks. The infrared of the glass system have various peaks which is related to different assignments like molecular weight around $3450cm^{-1}$ peak position, Asymmetric stretching relaxation of B-O bonds of trigonal BO_3 units at around ($1741\text{-}1636cm^{-1}$), vanadium content at $1530cm^{-1}$, Stretching vibration of B-O-V^{+5} and B-O-Pb^{+3} at around $952cm^{-1}$. The observed UV-visible absorption spectrum of BPV glass system show the $\pi - \pi^*$ electron transition band around 429-452 nm and also there is a shift to higher wavelength of the UV spectrum by increasing of vanadium oxide content. The optical band gap content in the two main optical transitions type (direct and indirect) while the refractive index of BPV glass system increased with increasing of the V_2O_5 content. When we study the real dielectric constant and imaginary dielectric constant, they have the same behavior which is stay constant value first then start to make hump then finally sudden increase of photon energy and the same behavior was for the optical conductivity. Finally, Photoluminescence shows the main peak at around 523.6nm and stock shift was at constant value [36].

Declaration of Competing Interest

The authors declare that they have no known competing financial interests or personal relationships that could have appeared to influence the work reported in this paper.

References

1. Gautam C, Yadav AK, Singh AK (2012) A Review on Infrared Spectroscopy of Borate Glasses with Effects of Different Additives. ISRN Ceram 1.

2. Abdelghany AM, Hammad AH (2015) Impact of vanadium ions in barium borate glass. Spectrochim Acta - Part A Mol Biomol Spectrosc 137: 39-44.

3. Moustafa MG, Shreif A, Ghalab S (2020) Towards superior optical and dielectric properties of borosilicate glasses containing tungsten and vanadium ions. Mater Chem Phys 254: 123464.

4. ElBatal HA, Hassaan MY, Fanny MA, Ibrahim MM (2017) Optical and FT Infrared Absorption Spectra of Soda Lime Silicate Glasses Containing nano Fe_2O_3 and Effects of Gamma Irradiation. Silicon 9: 511-517.

5. Motke SG, Yawale SP, Yawale SS (2002) Infrared spectra of zinc doped lead borate glasses. Bull Mater Sci 25: 75-78.

6. Naresh P, Naga Raju G, Gandhi Y, Piasecki M, Veeraiah N (2014) Insulating and Other Physical Properties of CoO-Doped Zinc Oxyfluoride-Borate Glass-Ceramics. J Am Ceram Soc 98(2): 413-422.

7. Agata G, Marta K, Wojciech AP, Joanna P (2020) Materials (Basel) 13, 5022.

8. Murugavel S, Roling B, (2007) Ion transport mechanism in borate glasses: Influence of network structure on non-Arrhenius conductivity. Phys Rev B – Condens Matter Mater Phys 76(18).

9. Henaish AMA, Abouhaswa AS (2020) Effect of WO_3 nanoparticle doping on the physical properties of PVC polymer. Bull Mater Sci 43.

10. Zhuang D, Lei S, Huang R, Yu G, Ma J (1992) Int Conf Lasers Optoelectron 1979: 88.

11. Haydar A (2012) Infrared Spectra and Energy band gap of Potassium Lithium Borate glass dosimetry. Int J Phys Sci 7: 922.

12. Alemi AA, Sedghi H, Mirmohseni AR, Golsanamlu V (2006) Synthesis and characterization of cadmium doped lead-borate glasses. Bull Mater Sci 29: 55-58.

13. EI Kamitsos, Patsis AP, Karakassides MA, Chryssikos GD (1990) Infrared reflectance spectra of lithium borate glasses. J Non Cryst Solids 126(1-2): 52-67.

14. El-Egili K, Doweidar H, Moustafa YM, Abbas I (2003) Structure and some physical properties of PbO–P_2O_5 glasses. Phys B Condens Matter 339(4): 237-245.

15. Saudi HA, Kameesy SUE (2019) Effect of barium addition and plasma nitriding treatment on chemical and physical properties of Al, Pb borate glass system as a developed radiation shield. J Phys Conf Ser 1253.

16. Henaish AMA, Mostafa M, Salem BI, Zakaly HMH, Issa SAM, et al. (2020) Spectral, electrical, magnetic and radiation shielding studies of Mg-doped Ni–Cu–Zn nanoferrites. J Mater Sci Mater Electron 31: 20210-20222.

17. Abdel Wahab EA, Shaaban KS, Elsaman R, Yousef ES (2019) Radiation shielding and physical properties of lead borate glass-doped ZrO_2 nanoparticles. Appl. Phys. A Mater Sci Process 125: 869.

18. Galeener FL, Lucovsky G, Mikkelsen JC (1980) Vibrational spectra and the structure of pure vitreous B_2O_3. Phys Rev B 22: 3983.

19. Som T, Karmakar B (2012) Antimony Charact Compd Appl 143.

20. Zakaly HMH, Rashad M, Tekin HO, Saudi HA, Issa SAM, et al. (2021) Synthesis, optical, structural and physical properties of newly developed dolomite reinforced borate glasses for nuclear radiation shielding utilizations: An experimental and simulation study. Opt Mater (Amst) 114: 110942.

21. Safonov IV, Rychagov MN, Kang K, Kim SH (2008) Adaptive sharpening of photos. Color Imaging XIII Process. Hardcopy Appl 6807: 68070U.

22. Abouhaswa AS, Perişanoğlu U, Tekin HO, Kavaz E, Henaish AMA (2020) Nuclear shielding properties of B2O3–Pb3O4–ZnO glasses: Multiple impacts of Er_2O_3 additive. Ceram Int 46(17): 27849-27859.

23. Jha P, Singh K, (2016) Effect of Field Strength and Electronegativity of CaO and MgO on Structural and Optical Properties of SiO_2–K_2O-CaO-MgO Glasses. Silicon 8: 437-442.

24. Alibwaini YA, Hemeda OM, El-Shater R, Sharshar T, Ashour AH (2021) Synthesis, characterizations, optical and photoluminescence properties of polymer blend PVA/PEG films doped eosin Y (EY) dye. Opt Mater (Amst) 111: 110600.

25. Venkatachalam S, Kanno Y, Mangalaraj D, Narayandass SK (2007) Effect of boron ion implantation on the structural, optical and electrical properties of ZnSe thin films. Phys. B Condens. Matter 390(1-2): 71-78.

26. Henaish AMA, El-Sharkawy AN, Shama SA, Hemeda OM, Ghazy R (2019) Structure and optical properties of nano $Ni_x Cd_{1-x} Fe_2O_4$ doped with optical dyes. J Phys Conf Ser 1253.

27. Das S, Madheshiya A, Ghosh M, Dey KK, Gautam SS, et al. (2019) Structural, optical, and nuclear magnetic resonance studies of V_2O_5-doped lead calcium titanate borosilicate glasses. J Phys Chem Solids 126: 17-26.

28. Henaish AMA, Issa SAM, Zakaly HMH, Tekin HO, Abouhaswa A (2021) Characterization of optical and radiation shielding behaviors of ferric oxide reinforced bismuth borate glass Phys Scr 96.

29. Abdullah M, Mohd W, Wan H, Kassim A, Yahya N (2019) Conf Pap, pp. 380.

30. Singh L, Thakur V, Punia R, Kundu RS, Singh A (2014) Structural and optical properties of barium titanate modified bismuth borate glasses. Solid State Sci 37: 64-71.

31. Laorodphan N, Pooddee P, Kidkhunthod P, Kunthadee P, Tapala W, et al. (2016) Boron and pentavalent vanadium local environments in binary vanadium borate glassesJ. Non Cryst Solids 453: 118-124.

32. Srinivas B, Hameed A, Srinivas G, Narasimha Chary M, Shareefuddin M (2021) Influence of V_2O_5 on physical and spectral (optical, EPR & FTIR) studies of SrO-TeO_2-TiO_2-B_2O_3 glasses. Optik (Stuttg) 225.

33. Kilic G, Ilik E, Mahmoud KA, El-Mallawany R, El-Agawany FI (2020) Novel zinc vanadyl boro-phosphate glasses: ZnO–V_2O_5– P_2O_5-B_2O_3: Physical, thermal, and nuclear radiation shielding properties. Ceram Int 46(11): 19318.

34. Abdelaziz TD, Ezzeldin FM, El Batal HA, Abdelghany AM (2014) Optical and FT Infrared spectral studies of vanadium ions in cadmium borate glass and effects of gamma irradiation. Spectrochim Acta - Part A Mol Biomol. Spectrosc 131: 497-501.

35. Depeursinge A, Racoceanu D, Iavindrasana J, Cohen G, Platon A, et al. (2010) Fusing visual and clinical information for lung tissue classification in high-resolution computed tomography. Artif Intell Med 50(1): 13-21.

36. Padlyak BV, Padlyak TB (2020) Spectroscopic properties of the V-doped borate glasses. J Non Cryst Solids 528: 119741.

Your next submission with JuniperPublishers
will reach you the below assets

- Quality Editorial service
- Swift Peer Review
- Reprints availability
- E-prints Service
- Manuscript Podcast for convenient understanding
- Global attainment for your research
- Manuscript accessibility in different formats
  (Pdf, E-pub, Full Text, Audio)
- Unceasing customer service

Track the below URL for one-step submission
https://juniperpublishers.com/submit-manuscript.php